Available online at www.eccomasproceedia.org
Eccomas Proceedia UNCECOMP (2017) 16-31

ECCOMAS
Proceedia

UNCECOMP 2017
2nd ECCOMAS Thematic Conference on
International Conference on Uncertainty Quantification in
Computational Sciences and Engineering
M. Papadrakakis, V. Papadopoulos, G. Stefanou (eds.)
Rhodes Island, Greece, 15–17 June 2017

OBTAINING HIGH ACCURACY VIBRATION MEASUREMENTS WITH LOW-COST SENSORS USING BAYESIAN VIRTUAL SENSING

Jyrki Kullaa

Department of Automotive and Mechanical Engineering
Metropolia University of Applied Sciences
P.O. Box 4021, 00079 Metropolia, Finland
e-mail: jyrki.kullaa@metropolia.fi

Keywords: Virtual Sensing, Bayes' Rule, Optimal Sensor Placement, Structural Dynamics, Response Estimation, Sensor Network.

Abstract. *Vibration measurements are utilized in many applications, e.g. structural health monitoring, vibration control, fatigue assessment, system identification, and model updating. Requirements for data accuracy are often high, which can be obtained by using high-quality sensors. However, wireless sensor networks often consist of a large number of low-cost sensor nodes, the accuracy of which may not fulfill the strict requirements of the applications.*

The possibility to replace high-quality vibration sensors with a larger number of low-cost sensors is studied. In order to achieve the required accuracy with low-cost sensors, empirical virtual sensing is introduced, which uses hardware redundancy for estimation. In empirical virtual sensing, the signal of a single sensor can be estimated from the data acquired by the whole sensor network. A Bayesian virtual sensor is derived, resulting in a posterior mean that is more accurate than the actual measurement provided the sensor noise is known. Also optimal sensor placement is studied to minimize the number of sensors.

Numerical simulations are performed for a structure subject to unknown random excitation. Noisy response is measured and the accuracy of virtual sensors is evaluated. Given the original reference sensor network with a small number of high-quality sensors, it is possible to determine the number of low-cost sensors needed to achieve the same accuracy. From this result, the cost-effectiveness can be assessed.

Peer-review under responsibility of the organizing committee of UNCECOMP 2017.
doi: 10.7712/120217.5348.16778

1 INTRODUCTION

Vibration measurements used in many applications, such as structural health monitoring, system identification, model updating, and vibration control, often require a sensor network with simultaneous sampling in order to capture the mode shape information at several locations of the structure. Traditionally, expensive high-quality accelerometers are used to acquire measurements with a high signal-to-noise ratio (SNR). A typical value of SNR in a measurement system is 30 dB. Excitation is often unknown, and response is only measured. Measured variables are usually accelerations, strains, displacements, or velocities.

With new technologies in intelligent structures and systems, digitalization, Internet of Things (IoT), MEMS sensors, and wireless sensor networks, an increasing number of sensors can be installed anywhere. Deployment of sensors is easy, because no cables are used, and the configuration of the sensor network is automatic. The sensor nodes have to be low-cost due to their large number in a single application. Therefore, the quality of the sensors may need to be compromised, which can result in a higher measurement error than with traditional high-quality sensors.

In the linear vibration theory, the structural response can be assumed to consist of the sum of modal contributions, in which only a few natural modes are active. With this assumption, a finite number of sensors is sufficient to make the sensor network redundant. The redundancy can be utilized to decrease the measurement error using virtual sensing techniques.

Virtual sensing (VS) can be either model-based (analytical) or data-driven (empirical) [1]. In analytical virtual sensing, in addition to measurement data, a finite element model is needed to estimate the unmeasured degrees of freedom. For example, full-field dynamic stress/strain field can be estimated using a limited number of sensors [2, 3].

Empirical virtual sensing is based on data from a redundant sensor network. It can be used, for example, to replace a temporarily installed or failed sensor [4]. Empirical virtual sensing has also been used for damage or sensor fault detection in structural health monitoring [5]. Also, combined empirical and analytical VS has been introduced for more accurate full-field response estimation than what can be obtained with analytical VS alone [6, 7].

In this study, empirical virtual sensing is applied to a large sensor network with low-cost sensors. The objective is to design a sensor network resulting in the same accuracy as a small number of high-quality sensors at the reference locations. It would then be possible to replace the original sensor network with a higher number of low-cost sensors. The quality of data is preserved and the decision between the two systems can be made with other criteria, e.g. hardware, installation, or maintenance costs.

The accuracy of the virtual sensors depends on the sensor locations. In order to minimize the required number of sensors, the sensors must be placed in optimal positions. Some review papers and comparisons of different optimal sensor placement (OSP) algorithms exist [8–11]. They present the most commonly applied algorithms and criteria. The sensor placement is a discrete optimization problem, for which genetic algorithms have been proposed [12–14]. Alternatively, a computationally efficient and widely used algorithm is to start with a large set of candidate sensor locations and removing one sensor in each round based on the selected criterion until the selected number of sensors remains. This backward sequential sensor placement (BSSP) algorithm has been used in many studies [15–17]. Another iterative method is to start with a small number of sensors and add one sensor in each round to the sensor network until the required criterion is fulfilled. The algorithm is called forward sequential sensor placement (FSSP) algorithm [13, 17, 18].

Iterative OSP algorithms are studied in this paper. First, a reference sensor configuration is designed using a widely used EFI method [15]. Three different OSP algorithms are studied

for virtual sensing. The cost function in the optimization is the error in the virtual sensors, which must be minimized under constrains concerning the number of sensors, types of sensors, possible locations of the sensors, etc. Bayesian analysis is applied to assess the estimation error. The sensor network must include the reference degrees of freedom (DOFs). The result is an optimal sensor network with a minimum number of sensors for the required accuracy.

It is assumed that measurements or simulations are available at all possible sensor locations and that measurement errors are Gaussian and known. The required input parameters include: (1) the candidate DOFs for sensors; (2) the virtual sensor DOFs (reference sensor network); (3) sensor noise information; (4) the criterion (cost function) for sensor network assessment; and (5) the stopping criterion, for example the desired accuracy or the number of sensors.

The paper is organized as follows. Empirical virtual sensing using Bayesian estimation is derived in Section 2. Optimal sensor placement for virtual sensing is discussed in Section 3. In Section 4, the method is validated by numerical simulations of ambient vibration measurements. Two types of physical and virtual sensors are studied. Concluding remarks are given in Section 5.

2 EMPIRICAL BAYESIAN VIRTUAL SENSING

Virtual sensing (VS), or soft sensing, is used to provide an alternative to physical measurement instrument. The quantity of interest is estimated using the available measurements and the system model. Virtual sensing can be classified into empirical and analytical techniques. Empirical VS is only studied in this paper.

Empirical virtual sensing is based on available current or historical measurements. Consider a sensor network measuring p simultaneously sampled variables $\mathbf{y} = \mathbf{y}(t)$ at time instant t. Each measurement $\mathbf{y}$ includes measurement error $\mathbf{w} = \mathbf{w}(t)$:

$$\mathbf{y} = \mathbf{x}_m + \mathbf{w} \tag{1}$$

where $\mathbf{x}_m = \mathbf{x}_m(t)$ are the exact values of the measured (m) degrees of freedom. All vectors are divided into predicted DOFs $\mathbf{u}$ and the remaining DOFs $\mathbf{v}$:

$$\mathbf{y} = \begin{matrix} \mathbf{y}_u \\ \mathbf{y}_v \end{matrix} \qquad \mathbf{x}_m = \begin{matrix} \mathbf{x}_{m,u} \\ \mathbf{x}_{m,v} \end{matrix} \qquad \mathbf{w} = \begin{matrix} \mathbf{w}_u \\ \mathbf{w}_v \end{matrix} \tag{2}$$

For simplicity but without loss of generality, assume zero-mean variables $\mathbf{y}$. The partitioned data covariance matrix $\mathbf{S}_y$ is

$$\mathbf{\Sigma}_y = E(\mathbf{y}\mathbf{y}^T) = \begin{matrix} \mathbf{\Sigma}_{y,uu} & \mathbf{\Sigma}_{y,uv} \\ \mathbf{\Sigma}_{y,vu} & \mathbf{\Sigma}_{y,vv} \end{matrix} = \begin{matrix} \mathbf{\Gamma}_{y,uu} & \mathbf{\Gamma}_{y,uv} \\ \mathbf{\Gamma}_{y,vu} & \mathbf{\Gamma}_{y,vv} \end{matrix}^{-1} = \mathbf{\Gamma}_y^{-1} \tag{3}$$

where the precision matrix $\mathbf{G}_y$ is defined as the inverse of the covariance matrix $\mathbf{S}_y$ and is also written in partitioned form. $E(\,)$ denotes the expectation operator.

A linear minimum mean square error (MMSE) estimate for $\mathbf{y}_u \mid \mathbf{y}_v$ ($\mathbf{y}_u$ given $\mathbf{y}_v$) is obtained by minimizing the mean-square error (MSE) and can be computed either using the covariance or precision matrix [5, 19]. The expected value, or the conditional mean, of the predicted variable is:

$$\hat{\mathbf{y}}_u = E(\mathbf{y}_u \mid \mathbf{y}_v) = -\mathbf{\Gamma}_{y,uu}^{-1}\mathbf{\Gamma}_{y,uv}\mathbf{y}_v \tag{4}$$

The error covariance MSE is

$$\mathrm{cov}(\mathbf{y}_u \mid \mathbf{y}_v) = \boldsymbol{\Gamma}_{y,uu}^{-1} \tag{5}$$

Although Equation 4 may give an accurate estimate, an even better estimate for $\mathbf{x}_{m,u}$ can be derived using Bayes' rule:

$$p(\mathbf{x}_{m,u} \mid \mathbf{y}) = p(\mathbf{x}_{m,u} \mid \mathbf{y}_u, \mathbf{y}_v) = \frac{p(\mathbf{y}_u \mid \mathbf{x}_{m,u}, \mathbf{y}_v) p(\mathbf{x}_{m,u} \mid \mathbf{y}_v)}{p(\mathbf{y}_u \mid \mathbf{y}_v)} \tag{6}$$

The three terms in Equation 6, the likelihood function, the prior distribution, and the evidence, are derived in the following. Measurement error $\mathbf{w}$ is assumed to be zero mean Gaussian, independent of $\mathbf{x}_m$, with a (known) covariance matrix

$$\boldsymbol{\Sigma}_w = E(\mathbf{w}\mathbf{w}^T) = \begin{bmatrix} \boldsymbol{\Sigma}_{w,uu} & \boldsymbol{\Sigma}_{w,uv} \\ \boldsymbol{\Sigma}_{w,vu} & \boldsymbol{\Sigma}_{w,vv} \end{bmatrix} \tag{7}$$

The likelihood in (6) is, according to (1) and (7):

$$p(\mathbf{y}_u \mid \mathbf{x}_{m,u}, \mathbf{y}_v) = p(\mathbf{y}_u \mid \mathbf{x}_{m,u}) = N(\mathbf{x}_{m,u}, \boldsymbol{\Sigma}_{w,uu}) \tag{8}$$

Using Equation 1 and the assumed noise model, the conditional means of $\mathbf{y}$ and $\mathbf{x}_m$ are equal:

$$E(\mathbf{x}_{m,u} \mid \mathbf{y}_v) = E(\mathbf{y}_u \mid \mathbf{y}_v) \tag{9}$$

Using Equations 1 and 7, the MMSE error covariance contains both the estimation error and noise:

$$\mathrm{cov}(\mathbf{y}_u \mid \mathbf{y}_v) = \mathrm{cov}(\mathbf{x}_{m,u} \mid \mathbf{y}_v) + \boldsymbol{\Sigma}_{w,uu} \tag{10}$$

The prior distribution is derived using (9) and (4):

$$p(\mathbf{x}_{m,u} \mid \mathbf{y}_v) = N(\mathbf{K}\mathbf{y}_v, \boldsymbol{\Sigma}_{\mathrm{prior},u}) \tag{11}$$

where $\mathbf{K} = -\boldsymbol{\Gamma}_{y,uu}^{-1}\boldsymbol{\Gamma}_{y,uv}$, and the prior covariance is obtained from (5) and (10):

$$\boldsymbol{\Sigma}_{\mathrm{prior},u} = \mathrm{cov}(\mathbf{x}_{m,u} \mid \mathbf{y}_v) = \boldsymbol{\Gamma}_{y,uu}^{-1} - \boldsymbol{\Sigma}_{w,uu} \tag{12}$$

The denominator $p(\mathbf{y}_u \mid \mathbf{y}_v)$ in (6) is the normalizing factor, which does not depend on $\mathbf{x}_{m,u}$. It is Gaussian with mean (4) and covariance (5), and could be easily evaluated. However, it is not necessary, because it is merely a scaling factor.

The posterior distribution (6) is derived by some manipulation, resulting also in a Gaussian distribution:

$$\begin{aligned} p(\mathbf{x}_{m,u} \mid \mathbf{y}) &= c_1 p(\mathbf{y}_u \mid \mathbf{x}_m) p(\mathbf{x}_{m,u} \mid \mathbf{y}_v) \\ &= c_2 \exp\left[-\frac{1}{2}(\mathbf{y}_u - \mathbf{x}_{m,u})^T \boldsymbol{\Sigma}_{w,uu}^{-1}(\mathbf{y}_u - \mathbf{x}_{m,u}) - \frac{1}{2}(\mathbf{x}_{m,u} - \mathbf{K}\mathbf{y}_v)^T \boldsymbol{\Sigma}_{\mathrm{prior},u}^{-1}(\mathbf{x}_{m,u} - \mathbf{K}\mathbf{y}_v) \right] \\ &= c_2 \exp\left[-\frac{1}{2}(\mathbf{x}_{m,u} - \hat{\mathbf{x}}_{m,u})^T \boldsymbol{\Sigma}_{\mathrm{post},u}^{-1}(\mathbf{x}_{m,u} - \hat{\mathbf{x}}_{m,u}) \right] \end{aligned} \tag{13}$$

where c_1 and c_2 are constants and the posterior covariance $\boldsymbol{\Sigma}_{\mathrm{post},u}$ is

$$\boldsymbol{\Sigma}_{\text{post},u} = \text{cov}(\mathbf{x}_{m,u} \mid \mathbf{y}) = (\boldsymbol{\Sigma}^{-1}_{w,uu} + \boldsymbol{\Sigma}^{-1}_{\text{prior},u})^{-1} \tag{14}$$

and the posterior mean is

$$\hat{\mathbf{x}}_{m,u} = E(\mathbf{x}_{m,u} \mid \mathbf{y}) = \boldsymbol{\Sigma}_{\text{post},u}(\boldsymbol{\Sigma}^{-1}_{w,uu}\mathbf{y}_u + \boldsymbol{\Sigma}^{-1}_{\text{prior},u}\mathbf{K}\mathbf{y}_v) \tag{15}$$

Notice that the posterior mean (15) is a weighted sum of the noisy measurement $\mathbf{y}_u$ and the MMSE estimate $\mathbf{K}\mathbf{y}_v$.

Equation 15 can also be written in the following matrix form.

$$\hat{\mathbf{x}}_{m,u} = E(\mathbf{x}_{m,u} \mid \mathbf{y}) = \begin{bmatrix}\boldsymbol{\Sigma}_{\text{post},u}\boldsymbol{\Sigma}^{-1}_{w,uu} & \boldsymbol{\Sigma}_{\text{post},u}\boldsymbol{\Sigma}^{-1}_{\text{prior},u}\mathbf{K}\end{bmatrix} \begin{matrix}\mathbf{y}_u \\ \mathbf{y}_v\end{matrix} = \mathbf{a}_u^T\mathbf{y} \tag{16}$$

where $\mathbf{a}_u^T$ is

$$\mathbf{a}_u^T = \begin{bmatrix}\boldsymbol{\Sigma}_{\text{post},u}\boldsymbol{\Sigma}^{-1}_{w,uu} & \boldsymbol{\Sigma}_{\text{post},u}\boldsymbol{\Sigma}^{-1}_{\text{prior},u}\mathbf{K}\end{bmatrix} \tag{17}$$

Generally, the predicted DOFs **u** may include several variables. In the sequel, **u** is one-dimensional including one sensor only. For each sensor *u*, a corresponding vector $\mathbf{a}_u^T$ is computed. All these vectors can be assembled in a coefficient matrix **A** to compute all estimates simultaneously:

$$\hat{\mathbf{x}}_m = \mathbf{A}\mathbf{y} \tag{18}$$

where each row *u* of matrix **A** represents the corresponding sensor. The rows corresponding to the reference sensor DOFs are only needed in this study.

3 OPTIMAL SENSOR PLACEMENT

In order to achieve the required accuracy of virtual sensors with a minimum number of physical sensors, the sensor locations must be optimized. The starting point is the reference sensor network with a small number of high-quality sensors. The objective is to replace this network with low-cost sensors using empirical virtual sensing.

Three algorithms are studied for optimal sensor placement: effective independence (EFI), backward sequential sensor placement (BSSP), and forward sequential sensor placement (FSSP).

EFI is a widely used algorithm, because no measurement data are needed but the mode shapes only. It has also shown to result in good results in many applications. However, it is not directly related to the accuracy of Bayesian virtual sensors. The effective independence vector is defined as (using a slightly modified expression from [16]):

$$E_D = \text{diag}\left[\boldsymbol{\Phi}_m(\boldsymbol{\Phi}_m^T\mathbf{W}\boldsymbol{\Phi}_m)^{-1}\boldsymbol{\Phi}_m^T\mathbf{W}\right] \tag{19}$$

where $\boldsymbol{\Phi}_m$ is the truncated modal matrix including the selected modes and the candidate measurement DOFs only. **W** is a weighting matrix defined as the inverse of the noise covariance matrix $\boldsymbol{\Sigma}_w$. The values of E_D represent the contributions of the corresponding sensor locations to the linear independence of the mode shape vectors in $\boldsymbol{\Phi}_m$. The sensor corresponding to the smallest value of E_D is removed and the E_D coefficients are then updated using the reduced modal matrix. The process is repeated iteratively until the number of sensors equals the required value.

The BSSP algorithm is iterative like EFI and it also starts with a large initial sensor network including all candidate DOFs. A single sensor is removed and the posterior variances are computed for the virtual sensors at the reference locations. The cost function is evaluated for the reduced sensor network. The cost function is evaluated for different sensor networks of the same number of sensors by removing each sensor in turn. Finally, the minimum cost is found, and the corresponding reduced sensor network is selected. The process is repeated until the required minimum accuracy is reached. Contrary to EFI, measurement data are needed but no mode shape information. The evaluated cost function is directly related to the accuracy of the virtual sensors. However, the optimal sensor placement may vary with different data sets, because the accuracy depends on the data covariance matrix $\mathbf{\Sigma}_y$ (3) that is estimated independently for each data set.

The FSSP algorithm is also iterative, starting with a small initial sensor network including only the reference DOFs. A single sensor is added and the posterior variances are computed for all virtual sensors at the reference locations. The cost function is evaluated for the expanded sensor network. The cost function is evaluated for different sensor networks of the same number of sensors by adding one sensor in turn. Finally, the minimum cost is found, and the corresponding expanded sensor network is selected. The process is repeated until the required accuracy is reached. The FSSP algorithm is a potential alternative, because in the present application an initial small reference sensor network is available, and the algorithm does not need to start from the scratch. In addition, FSSP can result in a dramatic reduction in the required computational effort [18].

The cost function used in this study is the error of the worst virtual sensor after removing (EFI, BSSP) or adding (FSSP) one sensor. Increasing the accuracy of the worst virtual sensor would finally result in the required accuracy of *all* virtual sensors.

4 NUMERICAL SIMULATIONS

4.1 Model and reference sensor network

An experiment was performed with a numerical model of a steel frame (Figure 1) with a height of 4.0 m and a width of 3.0 m. Both columns were fixed at the bottom. The frame was also supported with a horizontal spring at an elevation of 2.75 m with a spring constant of 2.0 MN/m. The frame was modelled with simple beam elements with hollow square cross section of 100 mm · 100 mm · 5 mm. The FE model consisted of 176 beam elements 62.5 mm in length and a single spring element.

Horizontal random loading was applied to the right column at nodes 113, 129, and 145, corresponding to elevations of 4 m, 3 m, and 2 m, respectively (Figure 1). The loads were mutually independent having standard deviations of 9 kN, 7 kN, and 5 kN, respectively. All load signals were low-pass filtered below 50 Hz.

Seven first modes were used in the simulation together with a static correction procedure [20]. Modal damping was assumed with a damping ratio of 0.01 for modes 1–2, 0.015 for mode 3, and 0.02 for modes 4–7.

The reference sensor network with a minimum number (7) of sensors was designed using the EFI method. The results are shown in Figure 1 both for acceleration and strain measurements. The same positions were also included in the new sensor network for virtual sensing.

Forced vibration was simulated and the response of all DOFs was recorded. One set of data was generated for accelerations and another for strains. Gaussian random noise was added to each sensor. The noise level was equal in all sensors and it was computed as follows. In the low-cost sensors, the average SNR was 21 dB in the network consisting of the reference

DOFs only. For acceleration measurements (case 1), it resulted in noise standard deviation of 9.47 m/s^2. For strain measurements (case 2), the noise standard deviation was 18.2 10^{-6}. The same data were used with all OSP algorithms.

Define the reference sensors and reference DOFs as the sensor network with high-quality sensors at the locations shown in Figure 1. Define the virtual sensors as the Bayesian estimates at the reference DOFs. Notice that the other locations for virtual sensing were ignored in this study.

The objective was to decrease noise in the virtual sensors by adding more sensors to the network. Three different accuracy requirements were studied: an increase of the average SNR by 3 dB, 6 dB, and 9 dB, which corresponded to average SNRs in the virtual sensors of 24 dB, 27 dB, and 30 dB, respectively. In acceleration measurements, they corresponded to the noise standard deviations of 6.71 m/s^2, 4.75 m/s^2, and 3.36 m/s^2, respectively. In strain measurements, the corresponding standard deviations of the noise were 12.9 10^{-6}, 9.10 10^{-6}, and 6.44 10^{-6}. These absolute standard deviations of the noise were used as the criteria for each sensor. Therefore, the resulted average SNRs probably exceeded the aforementioned values.

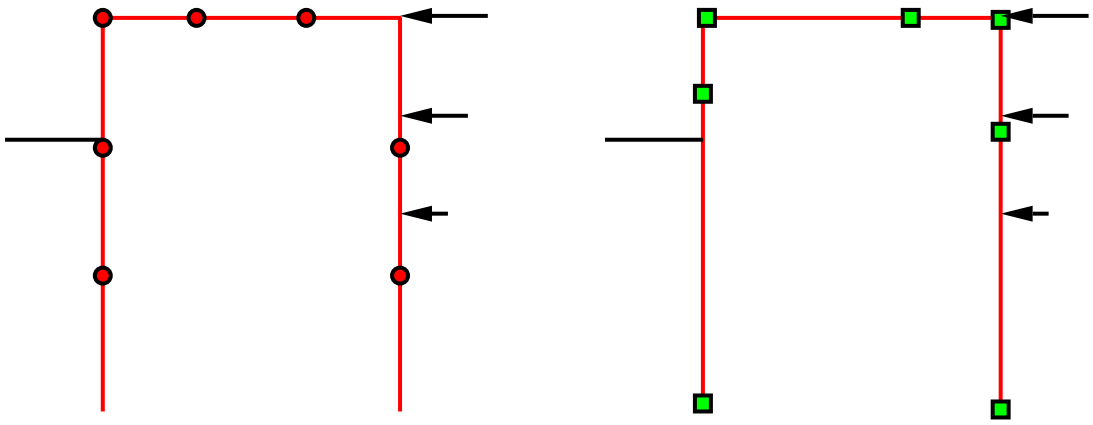

Figure 1: Finite element model of the frame structure with loads and reference sensor networks. The horizontal black line is the spring element. Left: accelerometers. Right: strain sensors.

4.2 Virtual accelerometers

In the first case, low-cost accelerometers were installed on the structure and the reference DOFs were estimated using empirical Bayesian VS. The average SNR of the sensors in the reference positions was 21 dB, and the objective was to study, how many sensors would be needed to increase the value of the virtual sensors to 24 dB, 27 dB, or 30 dB.

Three OSP algorithms were studied. First, the EFI method resulted in an increasing cost function with a decreasing number of sensors, as shown in Figure 2 left. Standard deviations of the estimation errors in the virtual sensors are shown in Figure 2 right for different number of sensors corresponding to the three required accuracy levels (the horizontal lines in the figure). The corresponding values of the cost function are shown with red circles in the left plot.

Starting from the top, the horizontal lines in Figure 2 right represent the physical sensors and the three criteria: average SNRs of 21 dB, 24 dB, 27 dB, and 30 dB, or equivalently, changes of the average SNR by 0 dB, +3 dB, +6 dB, and +9 dB of the virtual sensors compared to the physical measurements.

It can be seen that 12, 28, and 51 sensors were needed for an increase of the average SNR by 3 dB, 6 dB, and 9 dB, respectively. The sensor networks corresponding to those requirements are shown in Figure 3. It can be seen that all sensors had a tendency to be located at the reference locations. It should be noted that the same DOF was not allowed for multiple sensors.

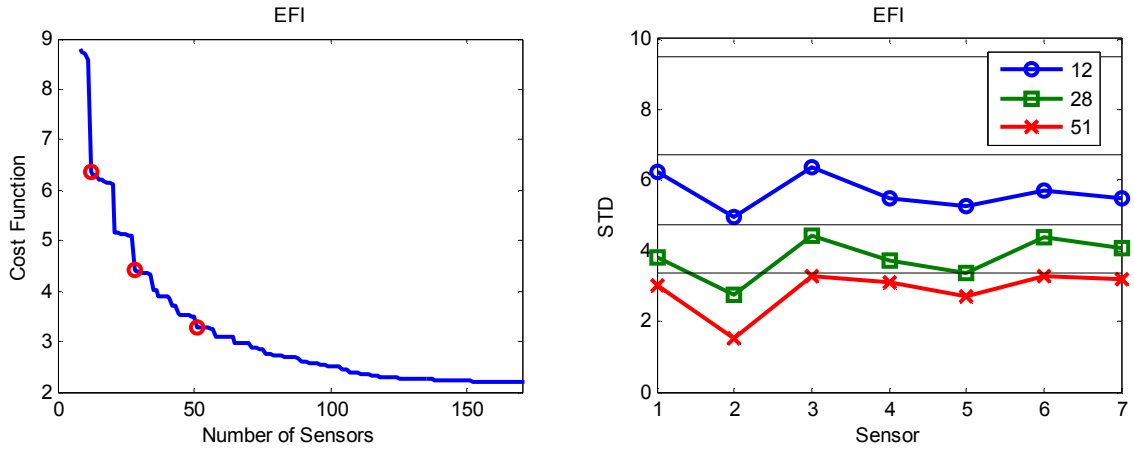

Figure 2: Optimal sensor placement using the EFI method. Left: Cost function with different number of sensors. Right: Standard deviations of the estimation errors in the virtual sensors with different number of sensors. The horizontal lines represent changes of the average SNR of the virtual sensors by 0 dB, +3 dB, +6 dB, and +9 dB compared to the physical measurements.

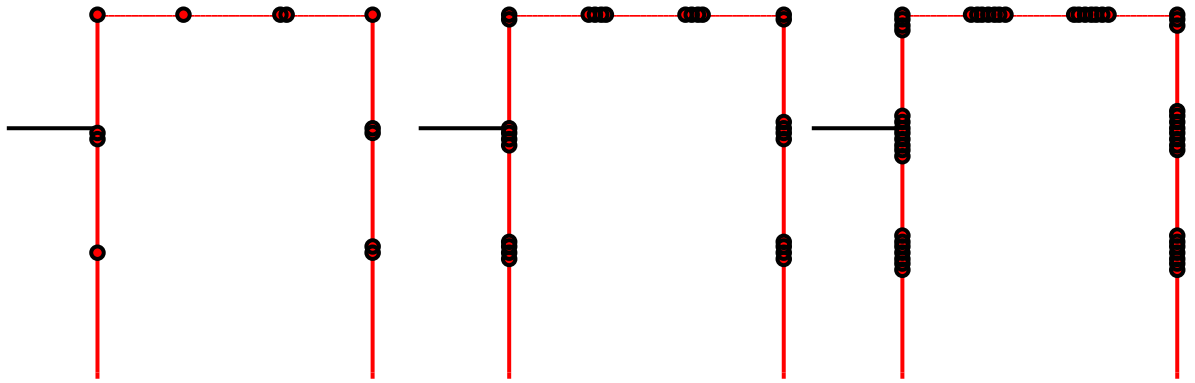

Figure 3: Optimal sensor placement using the EFI method. Sensor networks with 12, 28, and 51 accelerometers corresponding to increases of the average SNR of the virtual sensors by 3 dB, 6 dB, and 9 dB compared to the physical measurements.

In the BSSP algorithm, one sensor was removed in each round by minimizing the cost function, resulting in an increasing cost function with a decreasing number of sensors shown in Figure 4 left.

Standard deviations of the estimation errors in the virtual sensors are shown in Figure 4 right for different sensor networks fulfilling the given criteria. The corresponding values of the cost function are shown with red circles in the left plot. It can be seen that 10, 19, and 37 sensors were needed for an increase of the average SNR by 3 dB, 6 dB, and 9 dB, respectively. The sensor networks corresponding to those requirements are shown in Figure 5.

It can be seen that the sensors were more widely spread from the reference locations than when using the EFI method. Also, the same accuracy could be obtained with a smaller number of sensors than with the EFI method.

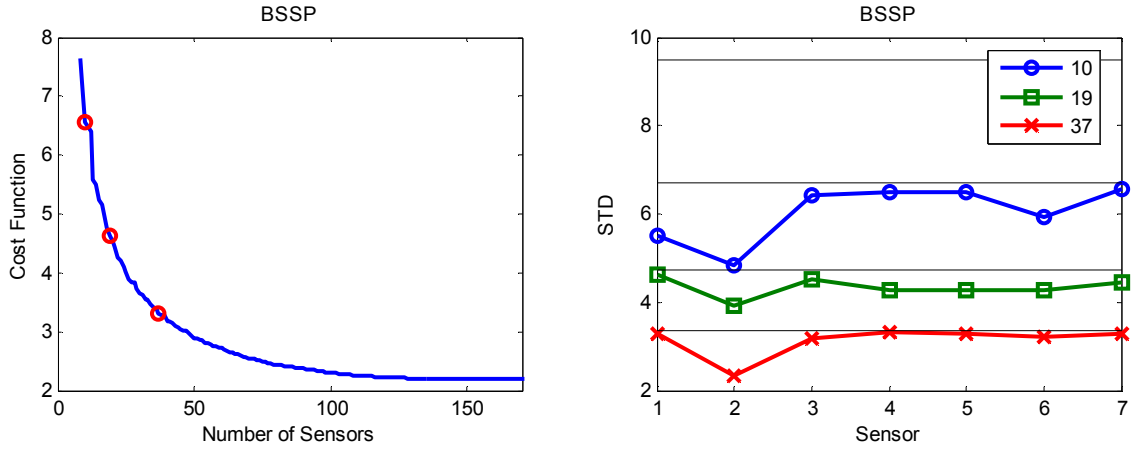

Figure 4: Optimal sensor placement using the BSSP algorithm. Left: Cost function with different number of sensors. Right: Standard deviations of the estimation errors in the virtual sensors with different number of sensors. The horizontal lines represent changes of the average SNR of the virtual sensors by 0 dB, +3 dB, +6 dB, and +9 dB compared to the physical measurements.

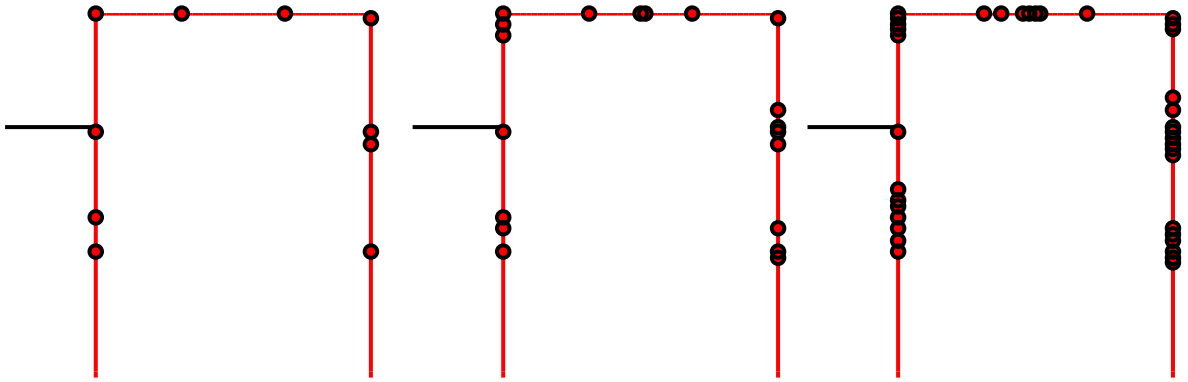

Figure 5: Optimal sensor placement using the BSSP algorithm. Sensor networks with 10, 19, and 37 accelerometers corresponding to increases of the average SNR of the virtual sensors by 3 dB, 6 dB, and 9 dB compared to the physical measurements.

In the FSSP algorithm, starting with the DOFs of the reference sensor network, one sensor was added in each round by minimizing the cost function, resulting in a decreasing cost function with an increasing number of sensors shown in Figure 6 left. The errors of all virtual sensors were evaluated and plotted in Figure 6 right for different number of sensors corresponding to the achieved criterion. The corresponding values of the cost function are shown with red circles in the left plot.

It can be seen that 12, 24, and 52 sensors were needed for an increase of the average SNR by 3 dB, 6 dB, and 9 dB, respectively. The sensor networks corresponding to those requirements are shown in Figure 7.

It can be seen that the sensors were more widely spread from the reference locations than when using the EFI or BSSP algorithms. In addition, the same accuracy could be obtained with a similar number of sensors as with the EFI method.

As a conclusion, the BSSP algorithm resulted in the highest accuracy with the least number of sensors. The difference between EFI and FSSP was not significant. They resulted in a similar number of sensors but placed in different positions.

Noise reduction of virtual sensor 2 in all algorithms was higher than what was required. Therefore, the resulted average SNRs of the virtual sensors were higher than the reported values.

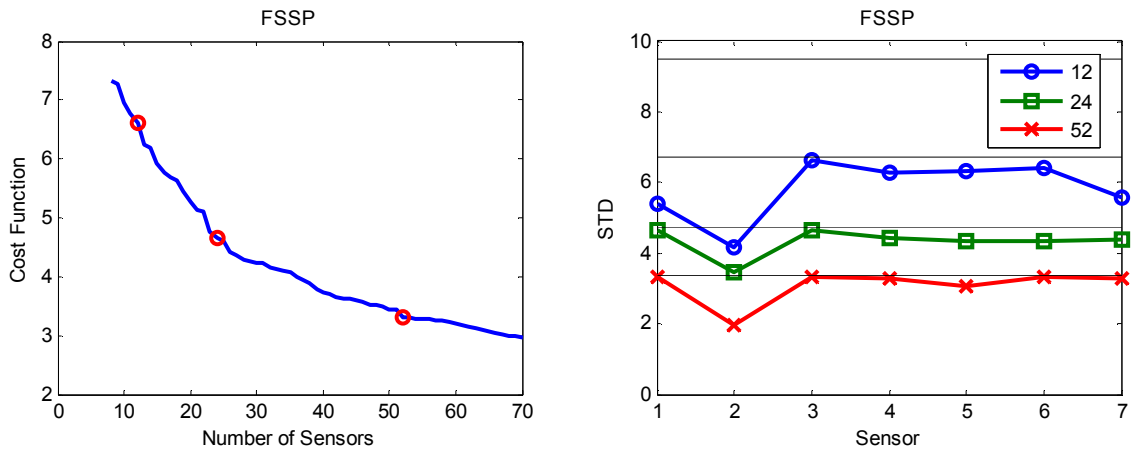

Figure 6: Optimal sensor placement using the FSSP algorithm. Left: Cost function with different number of sensors. Right: Standard deviations of the estimation errors in the virtual sensors with different number of sensors. The horizontal lines represent changes of the average SNR of the virtual sensors by 0 dB, +3 dB, +6 dB, and +9 dB compared to the physical measurements.

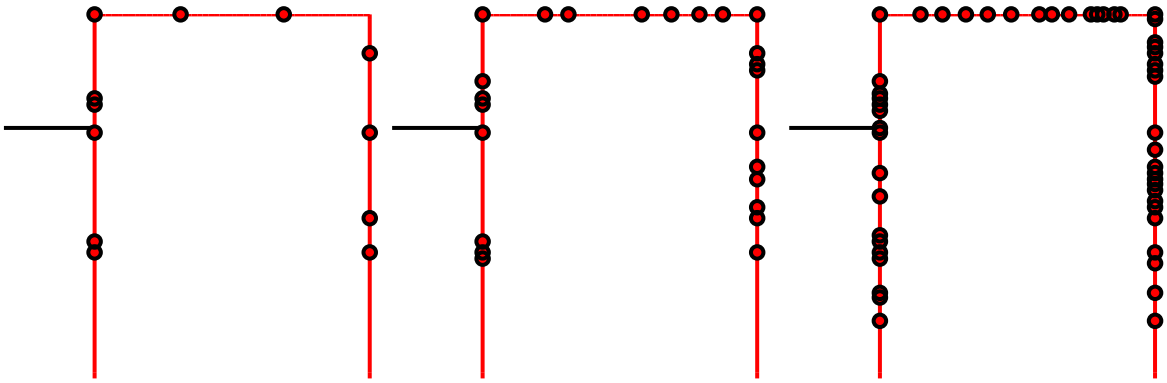

Figure 7: Optimal sensor placement using FSSP. Sensor networks with 12, 24, and 52 accelerometers corresponding to increases of the average SNR of the virtual sensors by 3 dB, 6 dB, and 9 dB compared to the physical measurements.

4.3 Virtual strain sensors

In the second case, the accuracy of virtual strain sensors at the reference DOFs was increased by adding more strain sensors in the network. The average SNR of the sensors in the

reference positions was 21 dB. The reference positions are shown in Figure 1 right. These DOFs were also included in the new sensor networks. The cost function was evaluated only at these reference locations.

First, the EFI method resulted in an increasing cost function with a decreasing number of sensors, as shown in Figure 8 left. Standard deviations of the estimation errors in the virtual sensors are shown in Figure 8 right for different number of sensors corresponding to the three required accuracy levels (the horizontal lines in the figure). Starting from the top, they represent the average SNRs of 21 dB, 24 dB, 27 dB, and 30 dB, or equivalently, an increase of the average SNR of 0 dB, +3 dB, +6 dB, and +9 dB compared to the physical measurements. The values of the cost function corresponding to the optimized sensor networks are shown with red circles in the left plot.

It can be seen that 13, 49, and 144 sensors were needed for an increase of the average SNR by 3 dB, 6 dB, and 9 dB, respectively. The sensor networks corresponding to those requirements are shown in Figure 9. It can be seen that the sensors were located in clusters. The same DOF was not allowed for multiple sensors. A very large number of sensors was needed for an increase of 9 dB. Sensors 1 and 7 seemed to be critical for the required accuracy (Figure 8 right).

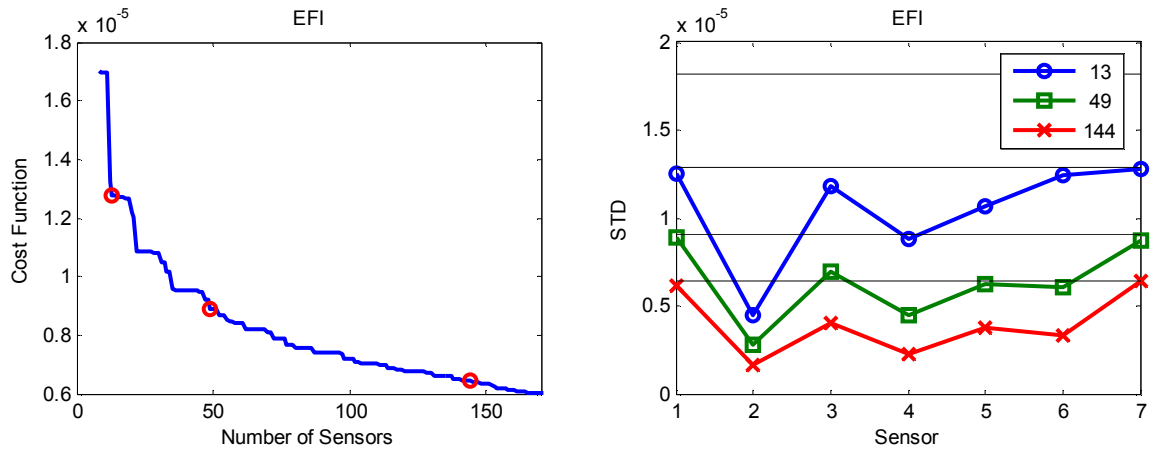

Figure 8: Optimal sensor placement using EFI. Left: Cost function with different number of sensors. Right: Standard deviations of the estimation errors in the virtual sensors with different number of sensors. The horizontal lines represent changes of the average SNR of the virtual sensors by 0 dB, +3 dB, +6 dB, and +9 dB compared to the physical measurements.

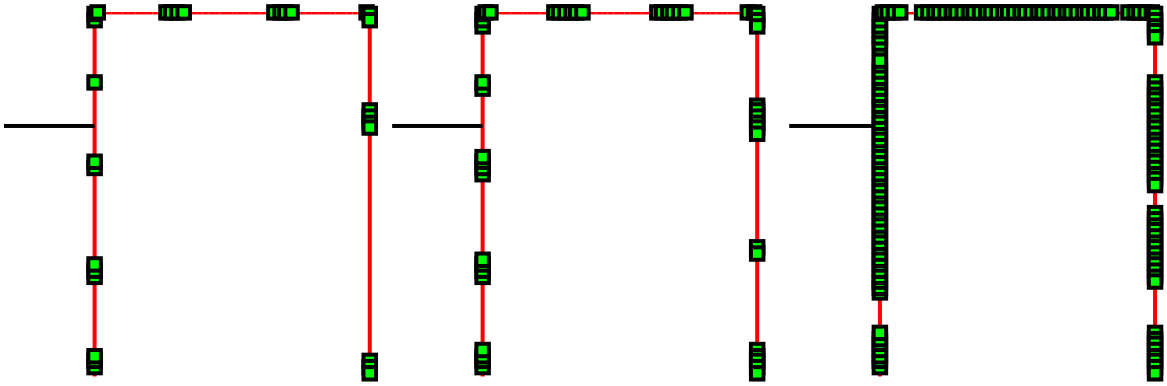

Figure 9: Optimal sensor placement using EFI. Sensor networks with 13, 49, and 144 strain sensors corresponding to increases of the average SNR of the virtual sensors by 3 dB, 6 dB, and 9 dB compared to the physical measurements.

The BSSP algorithm was started with all candidate sensor positions, and by removing a single sensor in each round resulted in increasing values of the cost function shown in Figure 10 left. Standard deviations of the estimation errors of all virtual sensors at the reference locations were computed and plotted in Figure 10 right for different sensor networks satisfying the given criteria. The corresponding values of the cost function are shown with red circles in the left plot.

It can be seen that 12, 27, and 78 sensors were needed for an increase of the average SNR by 3 dB, 6 dB, and 9 dB, respectively. The sensor networks corresponding to those requirements are shown in Figure 11.

It can be seen that the sensors were more widely spread from the reference locations than when using the EFI method. Also, the same accuracy could be obtained with a smaller number of sensors than with the EFI method. However, for the same increase in accuracy, the required number of strain sensors was much larger than that of accelerometers.

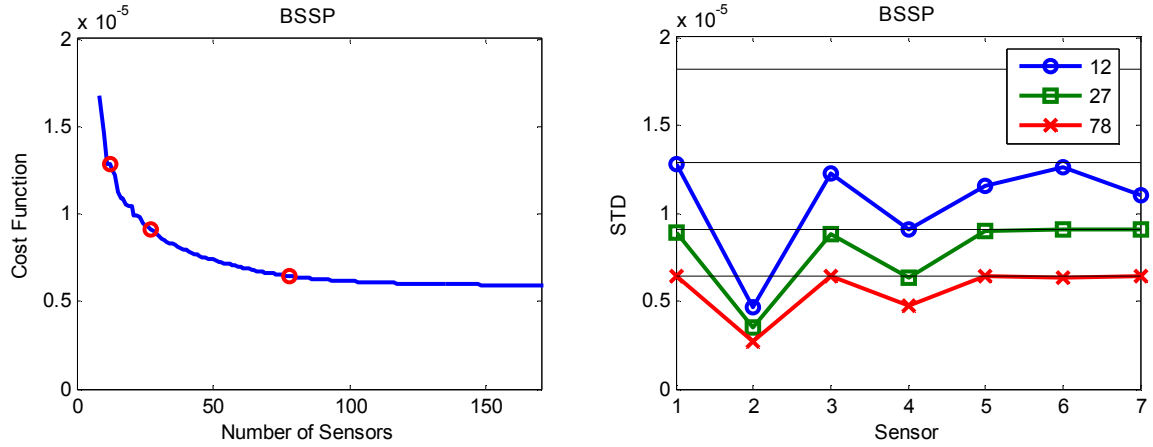

Figure 10: Optimal sensor placement using BSSP. Left: Cost function with different number of sensors. Right: Standard deviations of the estimation errors in the virtual sensors with different number of sensors. The horizontal lines represent changes of the average SNR of the virtual sensors by 0 dB, +3 dB, +6 dB, and +9 dB compared to the physical measurements.

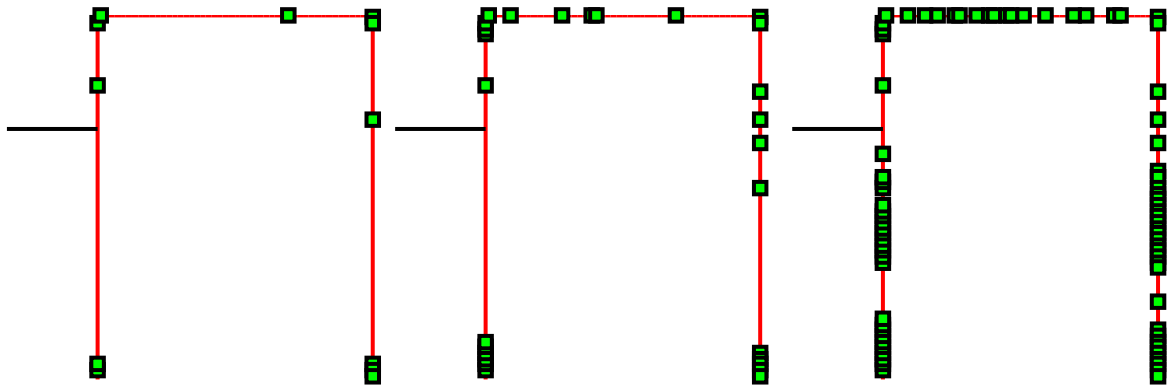

Figure 11: Optimal sensor placement using the BSSP algorithm. Sensor networks with 12, 27, and 78 strain sensors corresponding to increases of the average SNR of the virtual sensors by 3 dB, 6 dB, and 9 dB compared to the physical measurements.

The FSSP algorithm started with 7 strain sensors at the reference positions and added one sensor in each round so that the cost function was minimized. The decreasing cost function with an increasing number of sensors is shown in Figure 12 left.

Standard deviations of the virtual sensors at the reference DOFs are shown in Figure 12 right for different sensor networks fulfilling the given criteria. The corresponding values of the cost function are shown with red circles in the left plot.

It can be seen that 18, 39, and 83 sensors were needed for an increase of the average SNR by 3 dB, 6 dB, and 9 dB, respectively. The sensor networks corresponding to those requirements are shown in Figure 13.

It can be seen that the sensors were more widely spread from the reference locations than when using the EFI method. Also, the same accuracy could be obtained with a larger number of sensors than with BSSP but with a smaller number than with EFI.

As a conclusion, the BSSP algorithm resulted in the highest accuracy with the least number of sensors. EFI resulted in a much larger network than the other two algorithms. All methods yielded higher noise reduction in virtual sensors 2 and 4 than what was required.

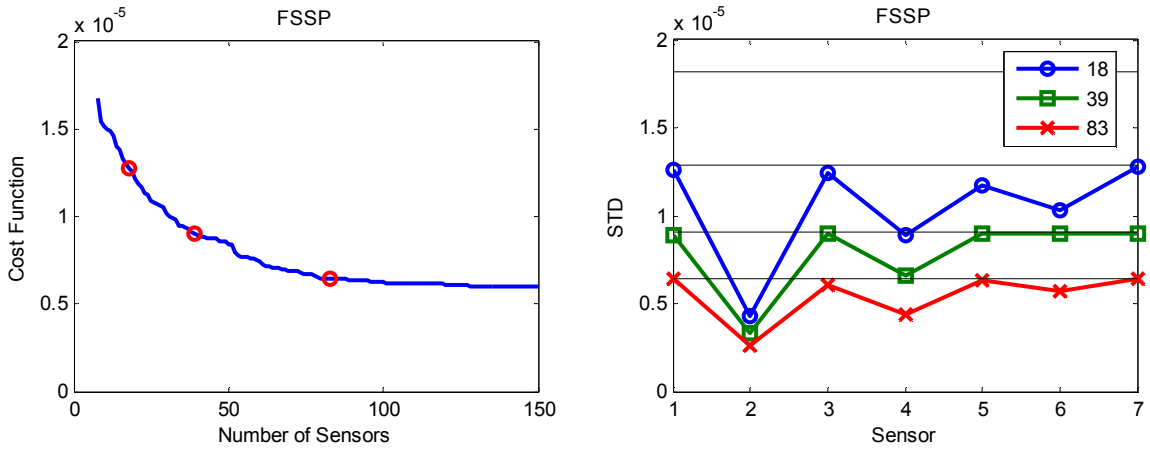

Figure 12: Optimal sensor placement using the FSSP algorithm. Left: Cost function with different number of sensors. Right: Standard deviations of the estimation errors in the virtual sensors with different number of sen-

sors. The horizontal lines represent changes of the average SNR of the virtual sensors by 0 dB, +3 dB, +6 dB, and +9 dB compared to the physical measurements.

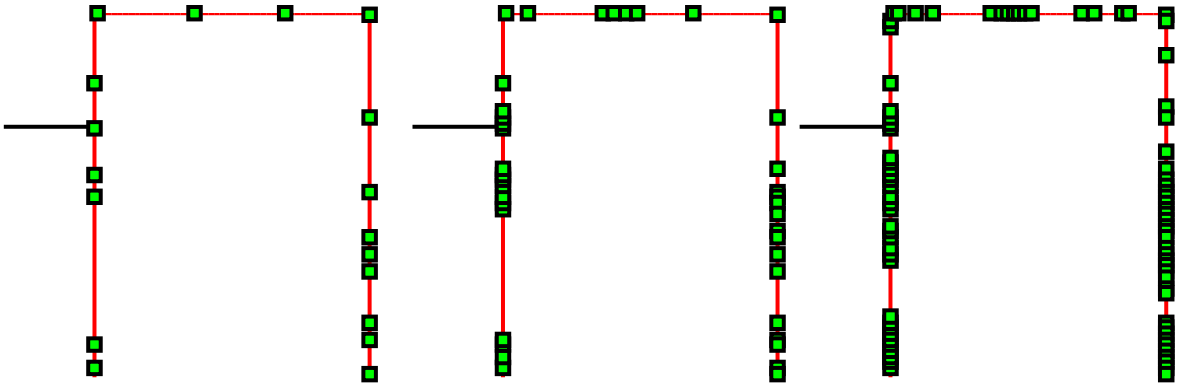

Figure 13: Optimal sensor placement using the FSSP algorithm. Sensor networks with 18, 39, and 83 strain sensors corresponding to increases of the average SNR of the virtual sensors by 3 dB, 6 dB, and 9 dB compared to the physical measurements.

As a summary, the number of sensors in the two cases using different OSP algorithms is shown in Table 1. It can be seen that increasing the accuracy by 3 dB could be done with just a few additional sensors, whereas the increase of 9 dB required very dense sensor networks. Another important result was that for the same accuracy increase, a smaller number of accelerometers was needed than strain sensors. In both cases, the BSSP algorithm showed the best performance.

Absolute	Change	Acceleration measurements			Strain measurements		
dB	dB	EFI	BSSP	FSSP	EFI	BSSP	FSSP
24	+3	12	10	12	13	12	18
27	+6	28	19	24	49	27	39
30	+9	51	37	52	144	78	83

Table 1: The number of acceleration or strain sensors needed for the required increase of the average SNR of virtual sensors using different OSP algorithms.

5 CONCLUSIONS

Empirical virtual sensing was studied in an application where low-cost sensors replace traditional high-quality sensors. The research question was that how many additional sensors would be needed to achieve the same accuracy as with a smaller number of high-quality sensors. It was shown that only a few additional sensors were needed to increase the SNR by 3 dB. However, in order to increase SNR by 9 dB, a dense sensor network would be needed.

BSSP was shown to be the best OSP algorithm in all cases. With EFI or FSSP, more sensors were needed for the same accuracy. For the same increase of the average SNR, the required number of accelerometers was smaller than that of strain sensors. The measurement error was assumed to be equal in all sensors. However, the resulting accuracy of the virtual sensors was not uniform. The cost function in the OSP algorithm was the maximum error of the worst sensor. Also other cost functions could be studied, e.g. the average error in the virtual sensors.

Also virtual sensors at other DOFs than the reference locations would be available. However, they were not used in this study, because the objective was to achieve the required accuracy only at the reference DOFs. This additional information could be useful in many applications.

The virtual sensors were estimated using measurement data. Because the excitation was random, different realizations would generally result in slightly different results. Therefore, it would be important to have different data sets to investigate the effect of excitation variability. Also the errors in the finite element model parameters were ignored. Empirical VS was based on the assumption that the noise was Gaussian and known. If noise is unknown, it is possible to use the MMSE estimate (4) instead, which yields accurate virtual sensors if the number of sensors is large enough.

REFERENCES

[1] B. Lin, B. Recke, J.K.H. Knudsen, S.B. Jørgensen, A systematic approach for soft sensor development. *Computers and Chemical Engineering,* **31**, 419–425, 2007.

[2] P. Pingle, P. Avitabile, Full-field dynamic stress/strain from limited sets of measured data. *Sound and Vibration*, 10–14, August 2011.

[3] E. Harvey, J. Ruddock, P. Avitabile, Comparison of full field strain distributions to predicted strain distributions from limited sets of measured data for SHM applications. B. Basu ed. *Tenth International Conference on Damage Assessment to Structures (DAMAS 2013)*, Dublin, Ireland, July 8–10, 2013.

[4] L. Liu, S.M. Kuo, M. Zhou, Virtual sensing techniques and their applications. *Proceedings of the 2009 IEEE International Conference on Networking, Sensing and Control*, Okayama, Japan, March 26–29, 2009.

[5] J. Kullaa, Sensor validation using minimum mean square error estimation. *Mechanical Systems and Signal Processing*, **24**, 1444–1457, 2010.

[6] J. Kullaa, Combined empirical and analytical virtual sensing in structural dynamics for uncertainty reduction. *1st ECCOMAS Thematic Conference on International Conference on Uncertainty Quantification in Computational Sciences and Engineering (UNCECOMP 2015)*, M. Papadrakakis, V. Papadopoulos, G. Stefanou (eds.), Crete Island, Greece, 25–27 May 2015.

[7] J. Kullaa, Combined empirical and analytical virtual sensing for full-field dynamic response estimation. *Proceedings of the 8th European Workshop on Structural Health Monitoring*. A. Güemes (ed.), Bilbao, Spain, July 5–8, 2016.

[8] T-H. Yi, H-N. Li, Methodology developments in sensor placement for health monitoring of civil infrastructures. *International Journal of Distributed Sensor Networks*, **2012**, 1550–1329.

[9] A. Krause, C. Guestrin, A. Gupta, J. Kleinberg, Near-optimal sensor placements: maximizing information while minimizing communication cost. *Proceedings of the 5th International Conference on Information Processing in Sensor Networks (IPSN '06)*, New York, NY, USA, 2–10, 2006.

[10] M. Meo, G. Zumpano, On the optimal sensor placement techniques for a bridge structure, *Engineering Structures*, **27**, 1488–1497, 2005.

[11] C. Leyder, E. Chatzi, A. Frangi, G. Lombaert, Comparison of optimal sensor placement algorithms via implementation on an innovative timber structure. *Life-Cycle of Engineering Systems: Emphasis on Sustainable Civil Infrastructure. Proceedings of the Fifth International Symposium on Life-Cycle Civil Engineering (IALCCE 2016)*. J. Bakker, D.M. Frangopol, K. van Breugel (eds.), 16–19 October, 2016, Delft, The Netherlands, 260–267.

[12] L. Yao, W.A. Sethares, D.C. Kammer, Sensor placement for on-orbit modal identification via a genetic algorithm. *AIAA Journal*, **31**, 1922–1928, 1993.

[13] C. Papadimitriou, Optimal sensor placement methodology for parametric identification of structural systems, *Journal of Sound and Vibration*, **278**, 923–947, 2004.

[14] K. Worden, A.P. Burrows, Optimal sensor placement for fault detection, *Engineering Structures* **23**, 885–901, 2001.

[15] D.C. Kammer, Sensor placement for on-orbit modal identification and correlation of large space structures, *Journal of Guidance, Control, and Dynamics*, **14**, 251–259, 1991.

[16] D.C. Kammer, Effects of noise on sensor placement for on-orbit modal identification of large space structures, *Journal of dynamic systems, measurements and control—Transactions of the ASCE*, **114**, 436–443, 1992.

[17] C. Papadimitriou, G. Lombaert, The effect of prediction error correlation on optimal sensor placement in structural dynamics, *Mechanical Systems and Signal Proce*ssing, **28**, 105–127, 2012.

[18] D.C. Kammer, Sensor set expansion for modal vibration testing. *Mechanical Systems and Signal Proce*ssing, **19**, 700–713, 2005.

[19] C.M. Bishop, *Pattern recognition and machine learning*. Springer, 2006.

[20] R.W. Clough, J. Penzien, *Dynamics of structures. 2nd edition*. McGraw-Hill, 1993.